



# Molecular dynamic investigations of aluminum nanoparticles coated by the mixtures of ethanol and diethyl ether with different molecular proportions

Pingan Liu · Penghua Sui · Zhichao Feng · Song Gao ·  
Naimeng Song · Ruochen Sun

Received: 9 April 2020 / Accepted: 4 August 2020 / Published online: 9 August 2020  
© Springer Nature B.V. 2020

**Abstract** Aluminum nanoparticles (ANPs) are considered energetic, economical, and eco-friendly additives. In this investigation, advanced ReaxFF molecular dynamics (MD) simulation has been used to discover the mechanism of coating ether and ethanol molecules on ANPs. Those MD results generally reveal the dynamics process of ethanol and ether adsorption. It is found that the adsorption of ethanol and ether molecules is not a physical adsorption process only. Newly generated aluminum-oxygen bonds are formed between oxygen atoms and aluminum atoms. Those oxygen atoms come from both ethanol and ether molecules. Moreover, ethanol and ether molecules generate ethyl and new ethanol molecules during the adsorption process. The radial distribution function curves and adsorption curves are used to describe the adsorption process. The results show that the adsorption amount of ethanol molecule is significantly higher than that of the ether molecule. It is observed that the outermost aluminum atoms form an

organic-provided alumina layer, the inside of ANPs is active aluminum atoms, and the outside is the organic coating layer. Heating could eliminate the hydrogen-bonding between solution molecules. High pressure and high temperature destroy the external structure of aluminum particles, which makes atoms migrate to the interior of aluminum particles. Finally, the oxidation resistance test shows that at 300 K, the organic coating layer can maintain good stability and oxidation resistance.

**Keywords** Molecular dynamic simulation · Aluminum · Nanoparticle · Coating · Energetic additives

## Introduction

Metal particles have been well applied as high energy carrier materials, due to good chemical stability and physical density (Sundaram et al. 2017). Compared with other metal materials, aluminum sources are abundant in nature. As a typical metal fuel, the energy density of aluminum is high, and its combustion products are nontoxic (Ab Wahid and Ali 2010; DeLuca 2018). Therefore, micro-sized aluminum particles have been widely used as additives in solid propellants (Marion et al. 1996). However, there are still such defects caused by the size limitation. In contrast to those large particles, ANPs have better reactivity, lower melting temperatures, and higher combustion rates, due to its high specific area and potential energy storage on the surface (Dreizin 2009; Yetter et al. 2009; Zha et al. 2014).

---

P. Liu · P. Sui · N. Song (✉) · R. Sun (✉)  
College of Aerospace and Civil Engineering, Harbin Engineering  
University, Nangang District, Harbin City, Heilongjiang Province,  
China  
e-mail: songnaimeng@hrbeu.edu.cn  
e-mail: sunrc836@hotmail.com

P. Liu  
Key Laboratory of Dual Dielectric Power Technology, Hebei  
Hanguang Industry Co., Ltd., Handan City, Hebei Province, China

Z. Feng · S. Gao  
Hua An Industry Group Co., Ltd, Nianzishan District, Qiqihar  
City, Heilongjiang Province, China

However, the limitation on the manufacture and storage of ANPs is still existing. Numerous studies showed that the drawback of ANPs' size was usually determined by the oxide coating on the surface of the particles under certain conditions (Yetter et al. 2009). It was reported that the alumina content of nanoparticles was much larger than that of micro-sized particles (Sundaram et al. 2015). As a result, alumina greatly reduces the energy content of nanoparticles (Chung et al. 2011), but bare ANPs cannot maintain their high reactivity in the air for a long period. Thus, it is of great significance to study surface coating materials for ANPs.

In the past, a variety of coating materials have been considered. One is metallic coating materials, which mainly include transition metals, metal oxides, and metal complexes (Foley et al. 2005; Sangeetha and Kalaignan 2015). ANPs coated with metallic coatings can be synthesized by wet chemical test method (Foley et al. 2005), electric explosion method (Gromov et al. 2006), and electroplating method (Lin et al. 2003). Another available type of coating material is organic. Considered as metal additives, ANPs covered by organic materials have better processability and compatibility (Sundaram et al. 2017). Therefore, many researchers have researched ANPs coated with organic materials. Ding et al. (2017) used poly (isobutyl vinyl ether) for chemical surface modification of alumina under low-temperature vacuum. Their experiments have proved that the formation of the coating improved the fluidity of the particles and extends the storage time of aluminum particles. Chung et al. (2009) studied the effect of epoxy compounds on the synthesis and passivation of ANPs. Their studies showed that 96% of the aluminum in the coated particles after passivation still had high activity. Besides, epoxy hexane- and epoxy dodecane-coated aluminum particles could remain stable in air.

Ethanol and ether serve commonly as solvents in the laboratory (Comyn 1997). Hydrogen bonds will be formed between molecules in an ethanol solvent due to the strong polarity of hydroxyl groups. Ethanol molecules produce aggregation due to hydrogen bonding. Ether solvent is a nonpolar solvent. A small number of hydrogen bonds can also be formed between ether and ethanol molecules, but the addition of ether increases the bonding distance of hydrogen bonds between ethanol molecules, which alleviates the aggregation between solution molecules. Besides, ethanol is an excellent liquid fuel. The addition of

ANPs in ethanol fuel significantly has been proved to reduce ignition delay time and increased combustion time (Gan and Qiao 2011; Tyagi et al. 2008). Comparing with conventional methods, MD simulations provide a novel solution for detailed microscopic studies at the molecular scale. Hong and van Duin (2015) studied the oxidation mechanism of ANPs by using the ReaxFF force field. Their results are in good agreement with the existing experimental literature on aluminum oxidation kinetics. Also, Zhang et al. (2018) investigated the oxidation of ANPs by ethanol using an MD simulation on the base of the ReaxFF force field. The simulation results showed good agreement with the first-principle calculations.

In this study, we select the mixture of ethanol and ether as coating materials for ANPs and chose MD simulation as the research method. The performance of ethanol and ether molecules on bulk aluminum materials with FCC crystal structure will be studied. Then, we study the adsorption process of annealed aluminum particles with 4 nm in diameter. We also discuss the changes in the adsorption process in molecular systems near the actual concentration with different molecular proportions and different temperature conditions, respectively. Finally, the oxidation resistance of the coating will be detected.

## Simulation methods and processes

### Research tools

Different from current experimental conditions, MD simulation uses Newton's classical mechanics to calculate the trajectories of multiple molecules in phase space, and which can be generally displayed as a function of time. The dynamic behavior of the molecule makes it easy to understand the evolution of coating behavior under certain conditions. During the coating process, the general force field may not be applicable because of the chemical bond breaking and hydrogenation reactions, ReaxFF force field can be a suitable choice (Senftle et al. 2016). ReaxFF uses a distance-dependent bond order function to represent the effect of chemical reactions on potential energy. The relationship between bond order and bond is the core of the ReaxFF potential. The bond order is determined by the distance between atoms and updates continuously during each MD simulation or energy minimization iteration. Now

ReaxFF force field is integrated as a USER-REAXC package in LAMMPS (Large-scale Atomic/Molecular Massively Parallel Simulator) (Aktulga et al. 2012). As a classic MD open-source program, LAMMPS was applied for all MD simulations in this study.

In this study, the ReaxFF force field file was developed by Van Duin et al. (Hong and van Duin 2015). This force field file contains atoms including aluminum, carbon, hydrogen, and oxygen. The total energy of the ReaxFF force field system has considered bond energy, over-coordinated energy, under-coordinated energy, lone pair energy, valence angle energy, torsional angular energy, Coulomb energy and Van der Waals energy. This force field file has been applied to describe Al–O bonds, Al–C bonds, Al–H bonds, and other aluminum-containing materials effectively (Hong and van Duin 2015; Hong and van Duin 2016). In our previous studies (Liu et al. 2018; Sun et al. 2019), the ReaxFF force field has been proven to simulate the reaction between ethanol, ether molecules, and aluminum atoms. Additionally, VMD (Humphrey et al. 1996) and OVITO (Stukowski 2010) programs are used as post-processing and visualization software, which also plays a critical role in the establishment of simulation data and analysis of simulation results.

CASTAP is a modern quantum mechanics basic program specially designed for solid materials science. It uses the density functional theory (DFT) plane-wave pseudopotential method to perform first-principles quantum-mechanical calculations. The typical applications include surface chemistry and bond structures (Bouhemadou et al. 2007a; Bouhemadou et al. 2007b; Chen et al. 2014).

### Simulation system and setup

This study includes two aluminum nanomaterials. One is block particles; the other is spherical particles. In Al nanomaterials with a crystal type of face-centered cube (FCC), tetrahedron interstice and octahedron interstice are independent of each other. Al block with (1 1 1) surface and (1 0 0) surface was set, which would give truncated octahedra. Due to the surface steps and kinks produced by cutting, spherical aluminum particles were annealed to eliminate the edge effect on the surface. The entire annealing process was performed under the canonical (NVT) ensemble. Berendsen method like a thermostat during the heating is the most efficient method to control the temperature. The damping constant was

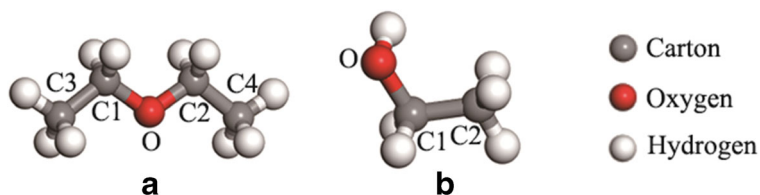
selected as 10 fs. ANPs were rapidly heated to 1200 K to ensure being melted completely. Next, the cooling process was carried out by the temperature decrement of 10 K. Particle is equilibrated for 10,000 steps at each temperature. The steepest descent method was selected to minimize the energy of particles. Finally, annealed aluminum particles are used as the initial configuration for subsequent simulations.

Ethanol and ether molecules are important adsorbates in this research. The molecular configuration was established by DFT calculations. The energy convergence tolerance was set to  $5 \times 10^{-6}$  eV/atom. Figure 1 shows the chemical configuration of ether and ethanol molecules. In the ReaxFF potential, the distance between the bonding atoms determines their relative energy and reaction. The bond lengths of ether and ethanol models are shown in Table 1.

For the case of studying nano-aluminum block, snapshots of the initial configuration are shown (Fig. 2a, b). The simulation box was set to  $40 \text{ \AA} \times 40 \text{ \AA} \times 65 \text{ \AA}$ . Aluminum block was located below the box, and ethanol and ether molecules were placed above  $6 \text{ \AA}$  from the Al surface. There were 30 ethanol molecules and 30 ether molecules randomly distributed in the box. The position distribution of these molecules was completed by the Packmol package (Martinez et al. 2009), which made it a stoichiometric mixture. All simulations were performed under the NVT ensemble. The time scale of the simulation is difficult to be consistent with that of the real experiment so that a larger temperature (kinetic energy) of solvent molecules is selected to facilitate the adsorption process. The temperature of the aluminum block was maintained at 300 K to avoid particle deformation caused by high temperature (Kornherr et al. 2006). The temperature of the ethanol and ether molecules was maintained at 500 K to speed up the simulation speed. At the beginning of the simulation, the simulated system was performed the energy minimization to ensure that the whole system stays in the ground state. A time step of 0.5 fs for  $2 \times 10^5$  iterations (up to 100 ps) was assigned because 0.5 fs describes the adsorption, dissociation, and diffusion of ethanol and ether molecules efficiently (Liu et al. 2019).

For the case of studying annealed ANPs, the simulation box was set up as a cubic box of  $80 \times 80 \times 80 \text{ \AA}$ , and annealed ANPs with a diameter of 4 nm were placed in the center of the box. In our simulations, 300 ethanol molecules and 300 ether molecules were randomly added in the box by the Packmol package, which made

**Fig. 1** Chemical structures for (a) ether and (b) ethanol molecular



it a stoichiometric mixture. A blank area of 7 Å was reserved between the coating solution molecules and the aluminum particles as a buffer area. A snapshot of the initial simulation system is shown (Fig. 2c). The simulation process of the ANPs case is the same as the case of nano-aluminum block. Differently, higher temperatures (700 K) were given to ethanol and ether molecules to make up for the deficiency of the simulation scale. The total running time length was about 100 ps. After the adsorption process, we cooled the system and then evaporated the excess ethanol and ether at low concentrations.

For the evaluations of coating, coated ANPs were placed in an oxygen environment. We also performed simulations of models with mixtures of different molecular proportions. For the specific setup, we will detail in the “Oxidation test for coated layer” section and the “Adsorption process of high concentration system” section.

## Results and discussion

### Reaction of ethanol and ether mixture over nano-aluminum block

Di Tommaso et al. (2011) revealed that a large number of ether molecules easily generate unstable peroxides

**Table 1** Bond lengths for ether and ethanol models

Molecular	Bond	$R_0$ (Å)
Ether	C–O	1.415
	C1–C3	1.513
	C1–H	1.108
	C3–H	1.098
Ethanol	C1–C2	1.519
	C–H	1.100
	C–O	1.436
	O–H	0.978

through autoxidation or peroxidation due to a self-propagating process of molecules. Liu et al. (2020) used MD simulations based on the ReaxFF force field to study the oxidation of ether over ANPs. We simulated the reaction of ethanol and ether molecules in a cubic box with dimensions of 40 Å × 40 Å × 40 Å. The results show that molecules can maintain their respective integrity in the mixed system. Moreover, the ethanol and ether molecules aggregated more significantly at low temperatures. This shows that heating can effectively inhibit the formation of hydrogen bonds between molecules during MD simulation, which is beneficial to the coating process of ANPs (Fig. 3).

We investigated the adsorption process of ethanol and ether mixed systems on nano-aluminum blocks. Figure 4 shows the snapshots of the adsorption process. At 1 ps, a few ethanol and ether molecules were adsorbed on the surface of the aluminum substrate. The number of molecules adsorbed gradually increases over time. Ether molecules tend to lay flat on the surface of particles, which have no fixed direction, but the ethanol molecules will gradually adjust their orientation so that the polar hydroxyl groups point to aluminum atoms. In addition, we have to consider the thermal vibrations of surface Al atoms due to the high temperature. It was found that the oxygen atoms of the ether molecules and the hydroxyl groups of the ethanol molecules were detached from the molecule when adsorbed on the Al surface. The oxygen and hydrogen atoms in the hydroxyl group would also be separated from each other. The separated atoms spread to the interior of the aluminum block surface to form new bond pairs. The minimal distance between the oxygen atom above the surface of the aluminum substrate and the surface aluminum atom is about 2.4 Å. The length of new Al–O bond pairs is about 1.9 Å. The remaining functional groups, such as ethyl, were present in the solution after atomic separation and adsorbed around aluminum atoms by Coulomb force, Van der Waals force, etc. The adsorption of ethanol and ether molecules affects the local charge of the aluminum atoms on the surface so

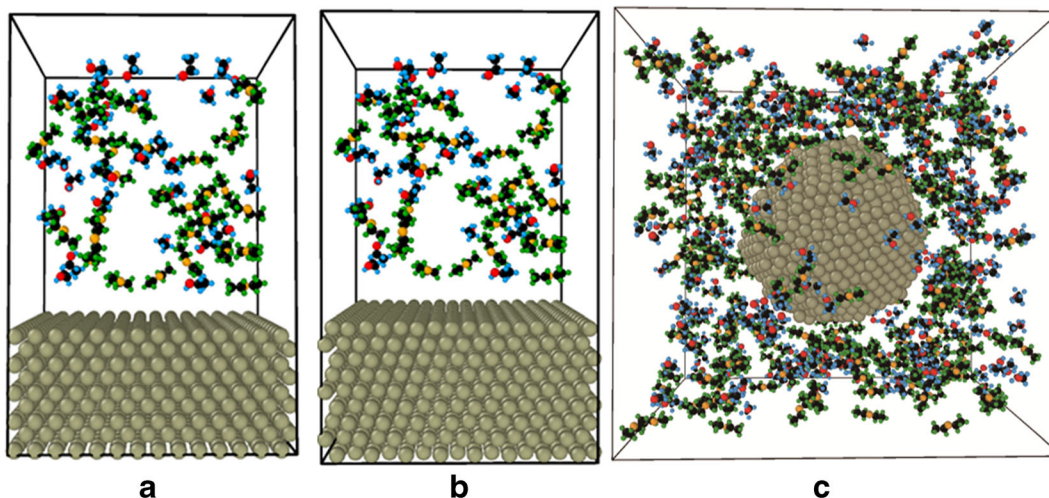


**Fig. 2** Initial configuration of nano-aluminum block with (1 0 0) surface case (a) and nano-aluminum block with (1 1 1) surface case (b). Annealed ANP case (c)

that these aluminum atoms show a positive charge (Fig. 4d). The formation of Al–O bonds causes the charge of Al atomic to the peak.

Compared with the aluminum block with (1 0 0) surface, (1 1 1) surface aluminum block arranged more closely at the same layers. Atoms in solution molecules are harder to get inside of Al particles. Figure 5 shows that the surface aluminum atoms show lower positive charges, which indicate fewer Al–O bonds are formed. This suggests that aluminum atoms on loose surfaces are more likely to form new bond pairs with solution molecules.

From the above analysis, we can conclude that ethanol and ether molecules can maintain the stability of their molecular properties in the mixed solution, respectively. During the adsorption process, we divide the adsorption methods into two methods. The first occurs

on the surface of aluminum substrate where the molecules adsorb on the surface through the Coulomb and Van der Waals forces. These molecules maintain their structure completely. The second occurs inside the aluminum substrate where new bond pairs formed between the atoms of the solution and aluminum atom. The residue continues can be adsorbed around the aluminum atom.

#### Adsorption mechanism on the bare ANPs

The “[Reaction of ethanol and ether mixture over nano-aluminum block](#)” section reveals that the adsorption of ethanol and ether molecules on the surface of aluminum particles is not simple physical adsorption. We are more interested in the adsorption process on anneal ANPs. In order to facilitate observation, the number of ethanol

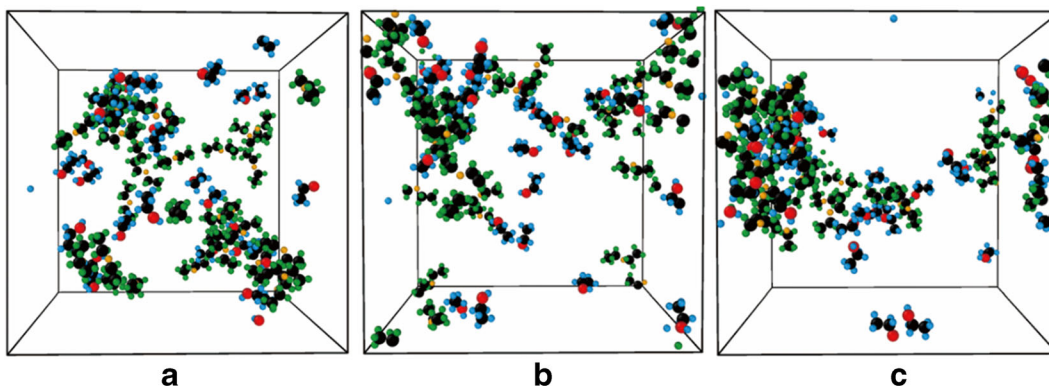
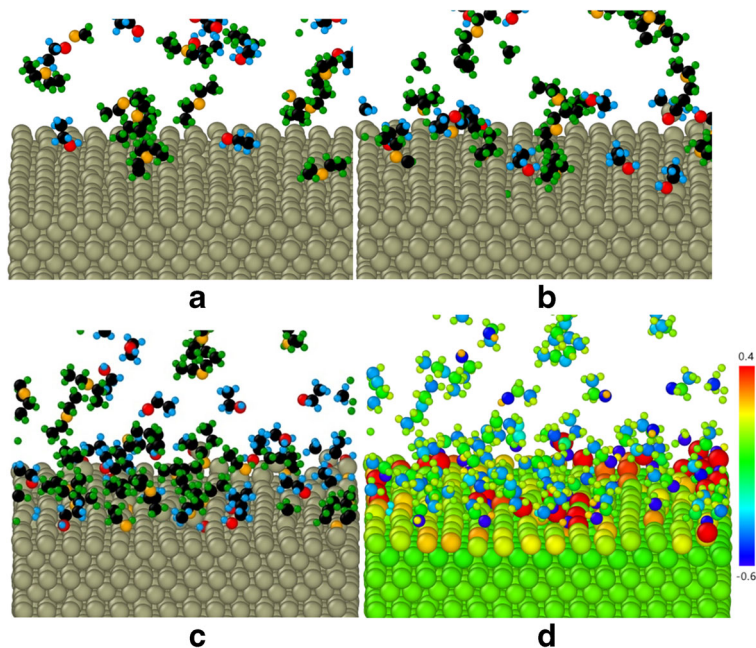


**Fig. 3** a Initial configuration. b Final configuration at 700 K. c Final configuration at 300 K of 30 ethanol molecules and 30 ether molecules in a simulation box measured as  $40 \text{ \AA} \times 40 \text{ \AA} \times 40 \text{ \AA}$

**Fig. 4** Snapshots illustrating an adsorption process of 30 ethanol molecules and 30 ether molecules on the aluminum substrate with (1 0 0) surface. **a** 1 ps, **b** 5 ps, **c** 25 ps, **d** 25 ps (colored by charge value)



and ether molecules added to the simulation box was controlled. A dense coating layer was formed on the ANPs' surface after adsorption (Fig. 6). Previous studies have shown that oxygen atoms play an important role in the adsorption process. We used the oxygen atoms as a characterization to count the number of ethanol and ether molecules within the 7 Å range of the ANPs' surface. Figure 6 shows the adsorption curves of ether/ethanol molecules on the surface of ANPs as a function of time. Initially, there are abundant free adsorption sites on the surface of ANPs. Ethanol and ether molecules can be quickly adsorbed on the surface of aluminum particles by two adsorption methods. The rate of adsorption curves gradually decreases due to the limitation of decreasing adsorption sites on the surface. Eventually, the number of adsorbed molecules will reach saturation values. In this simulation, the adsorption of ANPs on the

surface might not be complete because of the limitation of the number of solution molecules and the aggregation phenomenon. The method to solve this problem can use multiple coating cycles or increase the molecular density of the solution.

After the adsorption process, analyzing the structure of the solution and the coating layer on the surface of ANPs is very meaningful for the study. It is seen from the adsorption curve that the adsorbed number of ethanol molecules is significantly greater than that of ether molecules. We calculated the radial distribution function (RDF) between different atom pairs for further analysis. Figure 7 shows the RDF curves of the Al–O pairs formed by aluminum atoms and oxygen atoms of ethanol/ether molecules. The peaks of ethanol molecules are generally high. The polar hydroxyl groups of the ethanol molecules are more likely to be attracted by

**Fig. 5** Snapshots illustrating an adsorption process of 30 ethanol molecules and 30 ether molecules on the aluminum substrate with (1 1 1) surface. **a** 25 ps and **b** 25 ps (colored by charge value)

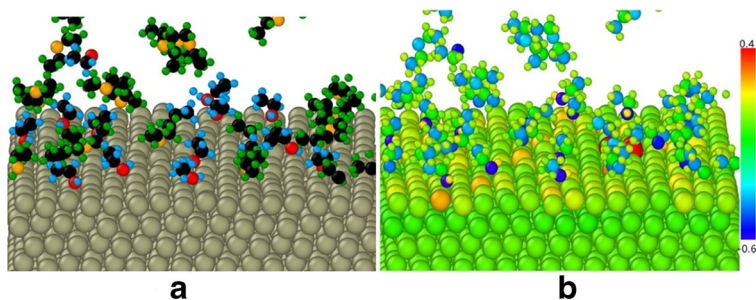
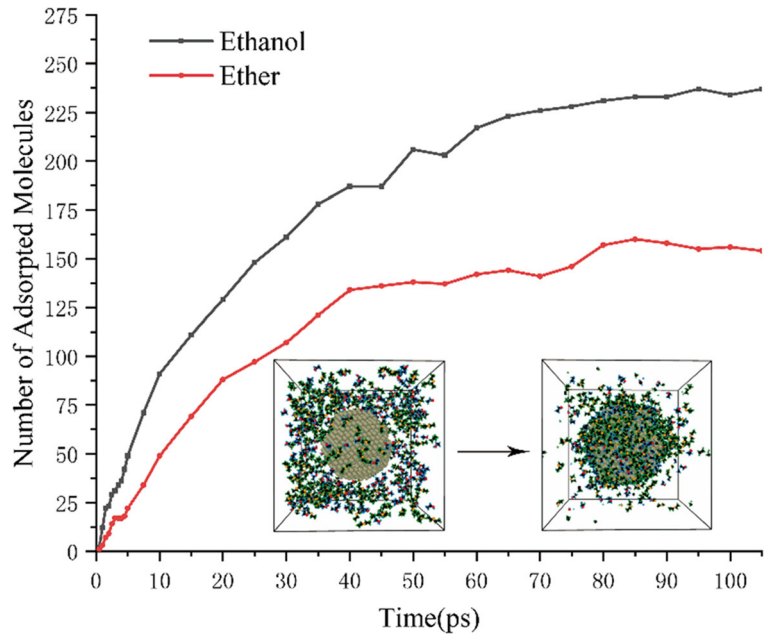


**Fig. 6** Adsorption curves of ether/ethanol molecules as a function of time and changes of their system configurations

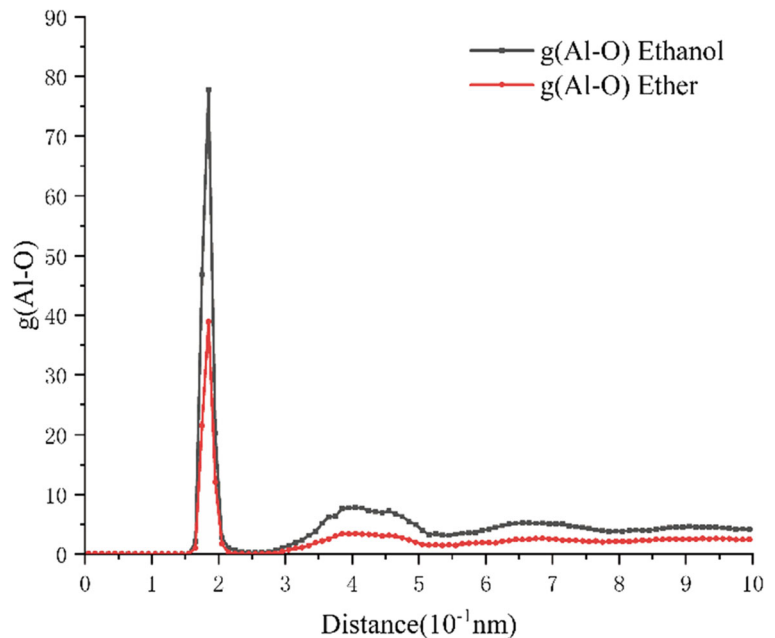


aluminum atoms. The length of the ethanol molecules is much shorter than the ether molecule. Therefore, ethanol molecules are prone to stacking, which is why the adsorbed number of ethanol molecules is more.

The first peak of the  $g(\text{Al-O})$  curve appears around 1.9 Å, which is consistent with the length of Al-O bond previously simulated on the aluminum substrate. This

data illustrates that the O atoms contacting with Al atoms closely are converted to Al-O bonds due to the rough surface of the annealing ANPs. Valley values appear at 2.1–2.9 Å, corresponding to the hydrocarbon group or other products left by the dissociation/ autoxidation of solution molecules. Subsequently, there are no large peaks on  $g(\text{Al-O})$  curves, which indicates

**Fig. 7** Radial distribution function curves of Al-O pairs formed by aluminum atom and the oxygen atom of ethanol/ether molecule



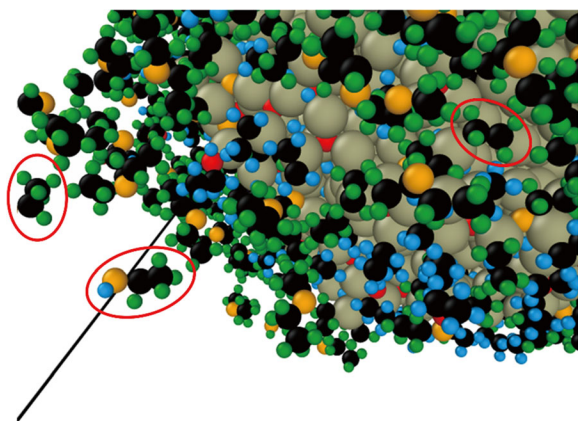


**Fig. 8** Ethanol and ethyl ether formed by ethanol/ether through a self-propagating process of autoxidation

that the molecules in the peripheral solution are relatively loose.

In the study of the “[Reaction of ethanol and ether mixture over nano-aluminum block](#)” section, we observed free ethyl groups. During the coating process of the annealed ANPs, we also observed the products in the dissociation/autoxidation of ether/ethanol molecules, such as ethanol and ethyl (Fig. 8). The follow-up showed that the reaction mechanism was consistent with the study by Di Tommaso et al. (2011). These products could be well adsorbed around ANPs. Eventually, no other products such as  $H_2$  and  $H_2O$  were found in the adsorption process which indicates that no strong chemical reaction occurred.

For the coated ANPs, we expect the internal aluminum atoms to remain highly active. Figure 9 shows the

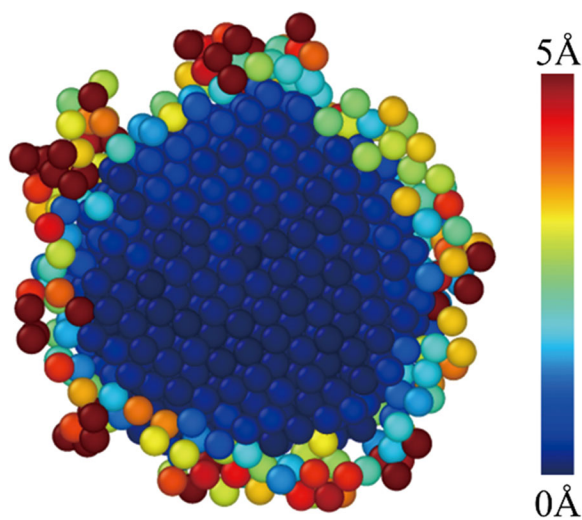


**Fig. 9** Final configuration colored by the Al atomic displacement

final configuration of aluminum atoms colored by the atomic displacement regarding the initial configuration. The atoms on the surface of ANPs move at a certain distance, while the internal aluminum atoms remain in the annealed structure. It is considered that the structure inside the aluminum particles remained stable. The surface of coated ANPs is saturated by the ethanol and ether molecules. The charge analysis of the final configuration shows interesting characteristics (Fig. 10). It is found that the outermost Al atoms in full contact with the ethanol and ether molecules show a positive charge due to the Al–O bonds built, which is considered to be a chemical adsorption layer. The negatively charged atoms distribute around the ANPs. Then, external atoms constituted the physical adsorption layer, which is adjacent to the adsorption layer due to the effect of Coulomb force and Van der Waals force. The charge of the internal Al atoms is lower than external Al atoms. It is considered that this part of aluminum atoms still maintains high reactivity.

#### Oxidation test for coated layer

After the adsorption process, we cooled the solution down to 300 K within 1 ps. Subsequently, we removed the unabsorbed ethanol and ether molecules. Using this method, we obtained a stable structure of the adsorption layer of ethanol and ether molecules. The density of oxygen is  $0.0014 \text{ g/cm}^3$  at standard atmospheric pressure. Considering the limitation of size and time scale in MD simulation, 200 oxygen molecules were randomly placed around the coated ANPs. Here, the density of oxygen was calculated as  $0.027 \text{ g/cm}^3$ . Snapshots of initial configuration and final simulation result are shown in Fig. 11.

We counted the number of adsorbed oxygen atoms during the oxidation process at 300 K (Fig. 12). After the simulation of 100 ps, the adsorbed oxygen atoms tend to a saturation value of approximately 220. We observed no  $H_2O$  and  $CO_2$  molecules generation during the oxidation process, which indicates that the integrity of the coating layer has not been damaged. We calculated the average distance between the adsorbed oxygen atoms and the center of the aluminum particles was  $23.98 \text{ \AA}$ . This distance is located in the range of the organic coating layer. From the above analysis, the coating layer shows good stability and oxidation resistance at 300 K.



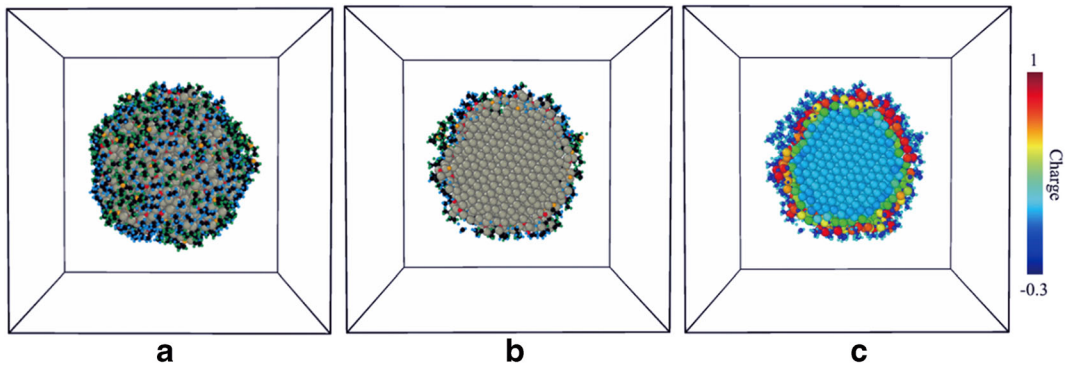


**Fig. 10** **a** Final configuration of the ANP coated by ethanol and ether molecules. **b** Cross-sectional view of the final configuration. **c** Cross-sectional view of final configuration colored by charge

**Fig. 11** **a** Initial configuration of 200 oxygen molecules and coated ANP. **b** The final configurations after the oxidation process at 300 K

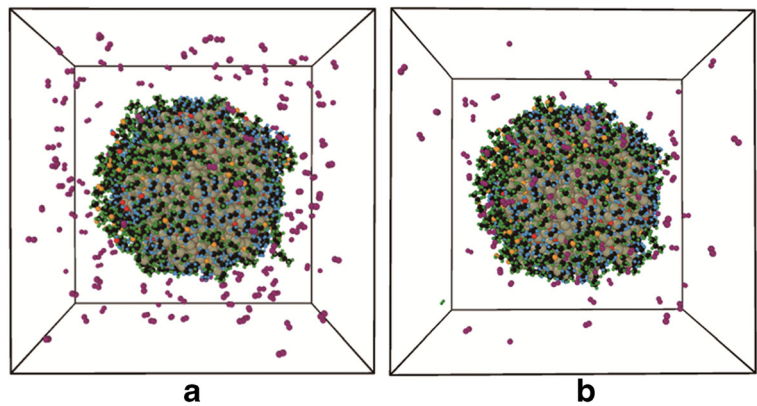


**Fig. 12** Number of absorbed oxygen atoms during the oxidation process

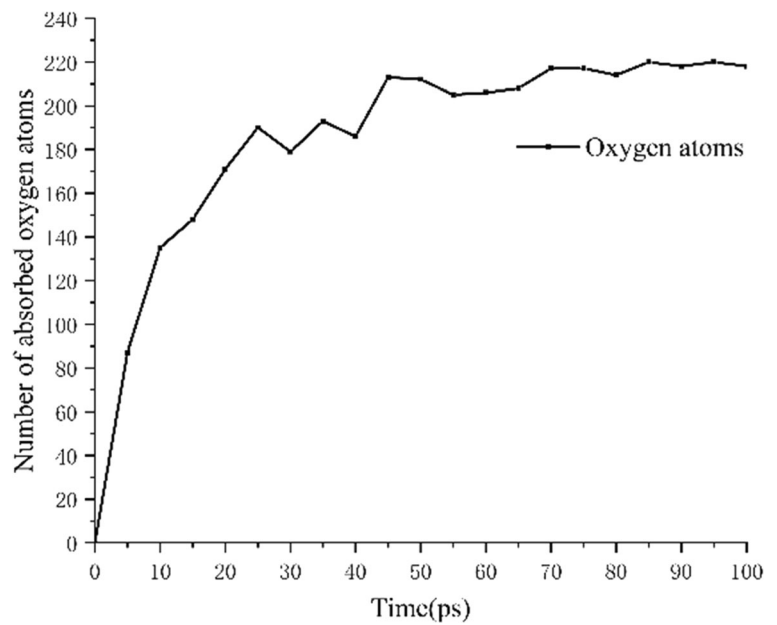


**Table 2** Parameter settings of eight initial adsorption simulation systems

Systems number	Content 1	Number of content 1	Content 2	Number of content 2	Temperature (K)
1#	Ethanol	1200	Ether	1200	500
2#	Ethanol	1200	Ether	1200	700
3#	Ethanol	1200	Ether	1200	900
4#	Ethanol	1200	Ether	1200	1100
5#	Ethanol	1480	Ether	920	500
6#	Ethanol	1480	Ether	920	700
7#	Ethanol	1480	Ether	920	900
8#	Ethanol	1480	Ether	920	1100

### Adsorption process of high concentration system

For the case of studying high concentration solutions, the simulation box was extended to  $90 \text{ \AA} \times 90 \text{ \AA} \times 90 \text{ \AA}$ . Table 2 summarizes the eight-initial system in the study of this section. Of all those systems, numbers 1# to 4# target the same molecular amount of ethanol and ether under different temperature conditions; numbers 5# to 8# are designed to the same mass of ethanol and ether under different temperature conditions. The density of ethanol solution is  $0.7893 \text{ g/cm}^3$  and that of ether solution is  $0.7364 \text{ g/cm}^3$ . As for pure solutions, it is expected that more than 6000 molecules of ethanol or more than 3600 molecules of ether will be needed to reach the level under standard conditions. In this study, there were 2400 solution molecules around the ANPs. Other simulation parameters are similar to the “[Adsorption mechanism on the bare ANPs](#)” section.

Figure 13 shows the snapshots of the final configuration after 1 ns of simulation in systems 1#–4#. It can

be seen that a large number of solution molecules aggregated. Since the adsorption effect, the aggregate formed by the ethanol and ether molecules was preferred around ANPs. Moreover, some atoms were observed to penetrate the outer layer of aluminum particles. The main reasons are as follows: (1) the number of ethanol and ether molecules in this study is relatively large. A large number of solution molecules form a high external pressure, which destroys the structure of the aluminum particles. (2) The aluminum particles selected in this study were annealed. The surface of aluminum particles is rough, resulting in some surface properties change. Atoms of solution molecules are easy to form new bond pairs with aluminum atoms on rough surfaces as discussed in the “[Reaction of ethanol and ether mixture over nano-aluminum block](#)” section. Through these analyses, we can imagine that the actual adsorption process will be more complicated.

Snapshots of the system configuration reveal that the aggregate of solution molecules becomes looser with increasing of temperature. The radial distribution function (RDF)  $g(r)$  is often used to analyze the structure of

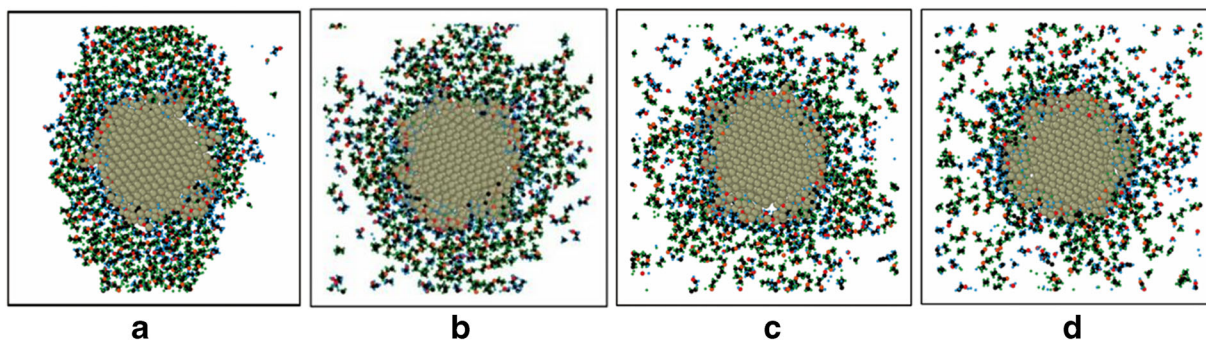


**Fig. 13** Snapshots of the final configuration of the ANPs coated with ethanol and ether molecules in the system 1#–4#. **a** system 1#, **b** system 2#, **c** system 3#, and **d** system 4#

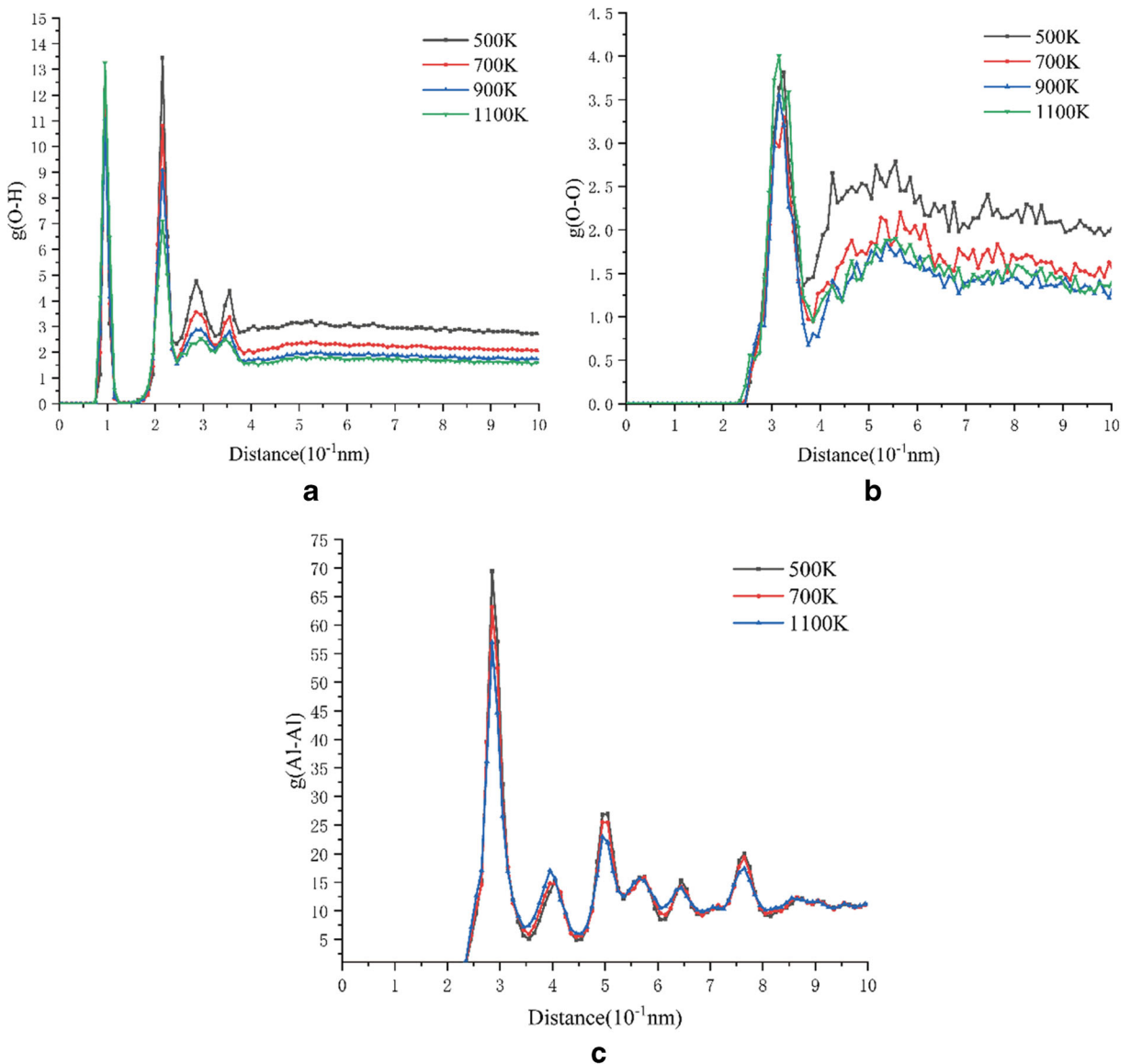


**Fig. 14** Radial distribution function curve of different atomic pairs. **a** O–H pairs, **b** O–O pairs, and **c** Al–Al pairs

the system (Fig. 14). The first highest peak of the  $g(\text{O}-\text{H})$  curve corresponds to hydroxyl groups. With the increase of temperature, the subsequent peak values decrease obviously. Moreover, the values of the  $g(\text{O}-\text{O})$  curve peaks show a downward trend in addition to the first peak. All of the above findings indicate that as the distance of the solution molecules increases, the structure of the system becomes loose. The effect of solution temperature on aluminum particles is also noteworthy. RDF is also used to reflect the structural information of aluminum particles. The first highest peak distance of the  $g(\text{Al}-\text{Al})$  curve represents the nearest

Al–Al bond length. The first peak decreases with increasing temperature, which indicates that the surface particle structure gradually changes from order to disorder. Hydrogen atoms and oxygen atoms are easier to diffuse inside the aluminum particle.

The adsorption curves of ether/ethanol molecules are shown in Fig. 15. Adsorption curves of ether molecules increase linearly within 25 ps and that of ether molecules within 50 ps. Their total adsorption quantities vary greatly. Compared with the “[Adsorption mechanism on the bare ANPs](#)” section, the adsorption rate and the number of adsorbed

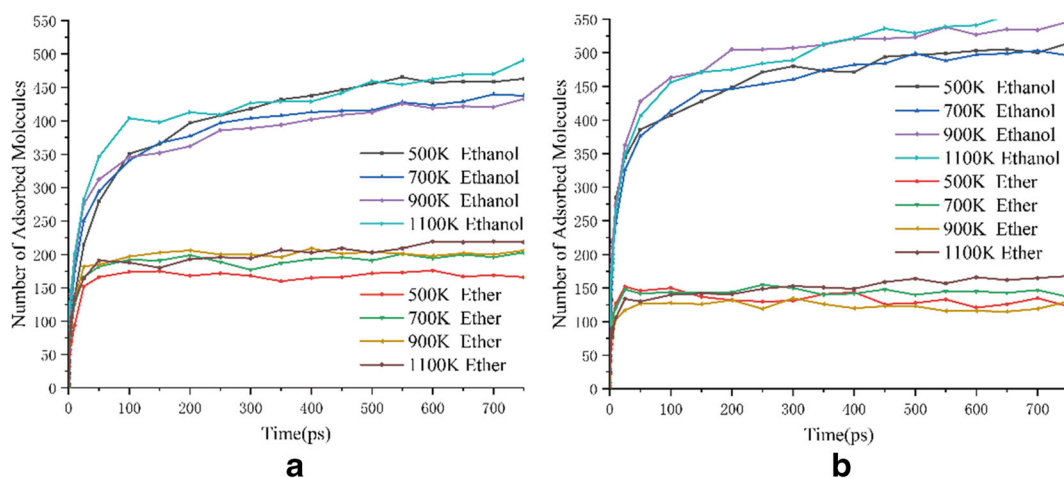


**Fig. 15** Adsorption curves of ether/ethanol molecules as a function of time. **a** Systems 1#–4#. **b** Systems 5#–8#

molecules are significantly increased by increasing the solution concentration. There is no obvious effect on the total adsorbed number during changed the two molecular quantity configurations, but the adsorbed number of ethanol/ether molecules is positively correlated with their concentration.

In previous studies, we observed that there was dissociation/autoxidation on solution molecules. We counted the composition information of the organic coating layer. The standard proportion values of each atom were calculated according to the chemical formula of ethanol molecule ( $C_2H_6O$ ) and ether molecule ( $C_4H_{10}O$ ). The result of Table 3 shows that the ratio of oxygen atoms in the coating layer is higher than the standard value. The snapshots of the final structure and the  $g(Al-H)$  and  $g(Al-C)$  curves of system 2# are also used to

demonstrate the dissociation/autoxidation on solution molecules (Fig. 16). Meanwhile, the product can be well adsorbed around the ANPs.

## Conclusion

In this study, we performed MD simulations with ReaxFF force field to uncover the coating process of ethanol and ether molecules on ANPs. The results show that coated ether molecules have no fixed direction, while the hydroxyl groups of ethanol molecules are always attracted by aluminum atoms and adsorbed on the aluminum particles. The thermal vibrations of surface Al atoms can cause the separation of atoms in solution molecules. Shorter Al–O bonds are formed between these

**Table 3** Composition information of organic coating layer

System	Coating material	Total adsorbed atoms	C (%)	H (%)	O (%)
Single	Ethanol	Standard value	22.2	66.7	11.1
1#		3661	21.8	65.6	12.6
2#		3519	22.3	65.3	12.4
3#		3342	21.6	65.5	12.9
4#		3380	20.3	65.2	14.5
Single	Ether	Standard value	26.7	66.7	6.7
1#		2342	26.4	66.5	7.1
2#		2583	26.7	65.5	7.8
3#		2546	26.3	65.6	8.1
4#		2481	25.4	65.8	8.8

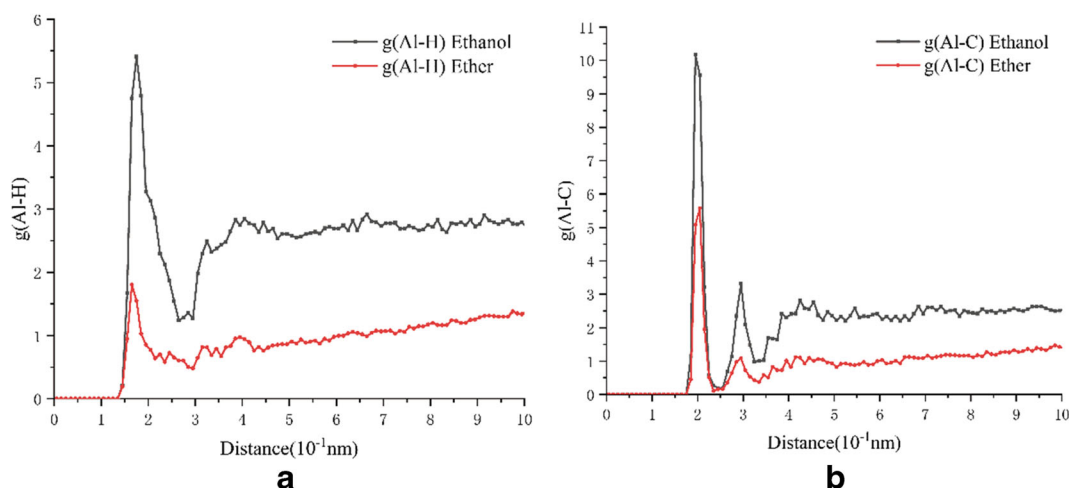


**Fig. 16** Radial distribution function curve of different atomic pairs in system 2#. **a** Al–H pairs. **b** Al–C pairs

oxygen atoms and aluminum atoms, especially on (1 0 0) surfaces. The surface of annealed aluminum particles generally presents loose, rough, and irregular shape. There are dissociation and autoxidation on ethanol and ether molecules, but the whole adsorption process is not a chemical reaction typically. Those reaction products can be well adsorbed around the aluminum particles. The adsorption amount of ethanol molecules is significantly higher than that of ether. From the analysis of system structure, we conclude that the outermost aluminum atoms tend to form an organic-provided alumina layer. The core of the particles is active aluminum atoms, and the outside is the organic coating layer. Oxidation tests show that the coating layer can maintain its integrity and protect aluminum particles from oxidation at 300 K.

For the study of high concentration solutions, it is found that the adsorption rate and the number of adsorbed molecules are both significantly higher than before. The adsorbed number of ethanol and ether molecules is positively correlated with the molecular concentration. High concentration generates high external pressure, which makes further H atoms, O atoms, and C atoms diffuse inside the nanoparticle more easily. High temperature can effectively eliminate hydrogen bonding nets between solution molecules. However, heating also makes the surface structure of aluminum particles more disordered. It provides more active reaction sites on the surface and therefore promotes the motion of oxygen atoms to the inside of the aluminum particles.

**Funding information** The present investigation was financially supported by the Fundamental Research Funds for Central Universities (3072020CFT0203).

**Compliance with ethical standards**

**Conflict of interests** The authors declare that they have no conflict of interest.

## References

- Ab Wahid M, Ali WKW (2010) Design and fabrication of a 200N thrust rocket motor based on  $\text{NH}_4\text{ClO}_4 + \text{Al} + \text{HTPB}$  as solid propellant. In: Wahid MA, Sherif JM, Sidik NAC, Samion S (eds) 10th Asian international conference on fluid machinery, vol 1225. AIP conference proceedings. Amer Inst Physics, Melville, pp. 1019–1026. doi:<https://doi.org/10.1063/1.3464841>
- Aktulga HM, Fogarty JC, Pandit SA, Grama AY (2012) Parallel reactive molecular dynamics: numerical methods and algorithmic techniques. *Parallel Comput* 38:245–259. <https://doi.org/10.1016/j.parco.2011.08.005>
- Bouhemadou A, Khenata R, Chegaar M (2007a) Structural and elastic properties of  $\text{Zr}_2\text{AlX}$  and  $\text{Ti}_2\text{AlX}$  ( $X = \text{C}$  and  $\text{N}$ ) under pressure effect. *Eur Phys J B* 56:209–215. <https://doi.org/10.1140/epjb/e2007-00115-6>
- Bouhemadou A, Khenata R, Chegaar M, Maabed S (2007b) First-principles calculations of structural, elastic, electronic and optical properties of the antiperovskite  $\text{AsNMg}_3$ . *Phys Lett A* 371:337–343. <https://doi.org/10.1016/j.physleta.2007.06.030>
- Chen JH, Long XH, Chen Y (2014) Comparison of multilayer water adsorption on the hydrophobic galena ( $\text{PbS}$ ) and hydrophilic pyrite ( $\text{FeS}_2$ ) surfaces: a DFT study. *J Phys Chem C* 118:11657–11665. <https://doi.org/10.1021/jp5000478>
- Chung SW et al (2009) Capping and passivation of aluminum nanoparticles using alkyl-substituted epoxides. *Langmuir* 25: 8883–8887. <https://doi.org/10.1021/la901822h>

- Chung SW, Gulians EA, Bunker CE, Jelliss PA, Buckner SW (2011) Size-dependent nanoparticle reaction enthalpy: oxidation of aluminum nanoparticles. *J Phys Chem Solids* 72:719–724. <https://doi.org/10.1016/j.jpms.2011.02.021>
- Comyn J (1997) Handbook of organic solvent properties. *Int J Adhesion Adhesives* 17:177. [https://doi.org/10.1016/S0143-7496\(97\)88687-3](https://doi.org/10.1016/S0143-7496(97)88687-3)
- DeLuca LT (2018) Overview of Al-based nanoenergetic ingredients for solid rocket propulsion. *Def Technol* 14:357–365. <https://doi.org/10.1016/j.dt.2018.06.005>
- Di Tommaso S, Rotureau P, Crescenzi O, Adamo C (2011) Oxidation mechanism of diethyl ether: a complex process for a simple molecule. *Phys Chem Chem Phys* 13:14636–14645. <https://doi.org/10.1039/c1cp21357a>
- Ding A, Hao J, Dong X, Huang J, Qian K, Ji S, Zhang Y, Li M (2017) Production, characterization, and flowability of assemblies consisting of highly active aluminum nanoparticles. *J Propuls Power* 33:1164–1169. <https://doi.org/10.2514/1.B36263>
- Dreizin EL (2009) Metal-based reactive nanomaterials. *Prog Energy Combust Sci* 35:141–167. <https://doi.org/10.1016/j.pecs.2008.09.001>
- Foley TJ, Johnson CE, Higa KT (2005) Inhibition of oxide formation on aluminum nanoparticles by transition metal coating. *Chem Mater* 17:4086–4091. <https://doi.org/10.1021/cm047931k>
- Gan YA, Qiao L (2011) Combustion characteristics of fuel droplets with addition of nano and micron-sized aluminum particles. *Combust Flame* 158:354–368. <https://doi.org/10.1016/j.combustflame.2010.09.005>
- Gromov A, Ilyin A, Forter-Barth U, Teipel U (2006) Characterization of aluminum powders: II. Aluminum nanopowders passivated by non-inert coatings. *Propellants Explos Pyrotech* 31:401–409. <https://doi.org/10.1002/prep.200600055>
- Hong S, van Duin ACT (2015) Molecular dynamics simulations of the oxidation of aluminum nanoparticles using the ReaxFF reactive force field. *J Phys Chem C* 119:17876–17886. <https://doi.org/10.1021/acs.jpcc.5b04650>
- Hong S, van Duin ACT (2016) Atomistic-scale analysis of carbon coating and its effect on the oxidation of aluminum nanoparticles by ReaxFF-molecular dynamics simulations. *J Phys Chem C* 120:9464–9474. <https://doi.org/10.1021/acs.jpcc.6b00786>
- Humphrey W, Dalke A, Schulten K (1996) VMD: visual molecular dynamics. *J Mol Graph Model* 14:33–38. [https://doi.org/10.1016/0263-7855\(96\)00018-5](https://doi.org/10.1016/0263-7855(96)00018-5)
- Kornherr A, Nauer GE, Sokol AA, French SA, Catlow CRA, Zifferer G (2006) Adsorption of organosilanes at a Zn-terminated ZnO (0001) surface: molecular dynamics study. *Langmuir* [1] 22:8036–8042. <https://doi.org/10.1021/la0604432>
- Lin JC, Jehng WD, Lee SL (2003) Electroplating of copper onto a preanodized 7005Al/Al<sub>2</sub>O<sub>3</sub>(P) metal matrix composite. *J Appl Electrochem* 33:597–605. <https://doi.org/10.1023/a:1024934014861>
- Liu J, Liu P, Wang M (2018) Molecular dynamics simulations of aluminum nanoparticles adsorbed by ethanol molecules using the ReaxFF reactive force field. *Comput Mater Sci* 151:95–105. <https://doi.org/10.1016/j.commatsci.2018.04.054>
- Liu PG, Sun RC, Qi H, Wang WC, Lv FW, Liu JP (2019) Molecular dynamic simulations of ether or ethanol coated aluminum nanoparticles for the application of hydrogenation: a comparison study. *Mater Res Express* 6:10. <https://doi.org/10.1088/2053-1591/ab221f>
- Liu J, Liu P, Wang M, Wang W, Lv F, Sun R, Yang Y (2020) Combustion of Al nanoparticles coated with ethanol/ether molecules by non-equilibrium molecular dynamics simulations. *Mater Today Commun* 22:2352–4928. <https://doi.org/10.1016/j.mtcomm.2019.100819>
- Marion M, Chauveau C, Gökalp I (1996) Studies on the ignition and burning of levitated aluminum particles\*. *Combust Sci Technol* 115:369–390. <https://doi.org/10.1080/00102209608935537>
- Martinez L, Andrade R, Birgin EG, Martinez JM (2009) PACKMOL: a package for building initial configurations for molecular dynamics simulations. *J Comput Chem* 30:2157–2164. <https://doi.org/10.1002/jcc.21224>
- Sangeetha S, Kalaignan GP (2015) Tribological and electrochemical corrosion behavior of Ni-W/BN (hexagonal) nanocomposite coatings. *Ceram Int* 41:10415–10424. <https://doi.org/10.1016/j.ceramint.2015.04.089>
- Senftle TP et al (2016) The ReaxFF reactive force-field: development, applications and future directions. *Npj Comput Mater* 2:14. <https://doi.org/10.1038/npjcompumats.2015.11>
- Stukowski A (2010) Visualization and analysis of atomistic simulation data with OVITO—the Open Visualization Tool Model. *Simul Mater Sci Eng* 18:7. doi:<https://doi.org/10.1088/0965-0393/18/1/015012>
- Sun R, Liu P, Qi H, Liu J, Ding T (2019) Molecular dynamic simulations of ether-coated aluminum nanoparticles as a novel hydrogen source. *J Nanopart Res* 21:15. <https://doi.org/10.1007/s11051-019-4513-6>
- Sundaram DS, Yang V, Zarko VE (2015) Combustion of nano aluminum particles (Review). *Combust Explos* 51:173–196. <https://doi.org/10.1134/s0010508215020045>
- Sundaram D, Yang V, Yetter RA (2017) Metal-based nanoenergetic materials: synthesis, properties, and applications. *Prog Energy Combust Sci* 61:293–365. <https://doi.org/10.1016/j.pecs.2017.02.002>
- Tyagi H, Phelan PE, Prasher R, Peck R, Lee T, Pacheco JR, Arentzen P (2008) Increased hot-plate ignition probability for nanoparticle-laden diesel fuel. *Nano Lett* 8:1410–1416. <https://doi.org/10.1021/nl080277d>
- Yetter RA, Risha GA, Son SF (2009) Metal particle combustion and nanotechnology. *Proc Combust Inst* 32:1819–1838. <https://doi.org/10.1016/j.proci.2008.08.013>
- Zha M, Lv X, Ma Z, Zhang L, Zhao F, Xu S, Xu H (2014) Effect of particle size on reactivity and combustion characteristics of aluminum nanoparticles. *Combust Sci Technol* 187:1036–1043. <https://doi.org/10.1080/00102202.2014.1001510>
- Zhang YR, van Duin ACT, Luo KH (2018) Investigation of ethanol oxidation over aluminum nanoparticle using ReaxFF molecular dynamics simulation. *Fuel* 234:94–100. <https://doi.org/10.1016/j.fuel.2018.06.119>

**Publisher's note** Springer Nature remains neutral with regard to jurisdictional claims in published maps and institutional affiliations.